


RESEARCH

Open Access



Comparative analysis of eco-epidemic model with disease in prey and gestation delay in predator: implications for population dynamics

Bipin Kumar^{1*} , Rajesh Kumar Sinha¹ and Saddam Hussain²

*Correspondence:

bipink.ph21.ma@nitp.ac.in

¹Department of Mathematics,
National Institute of Technology
Patna, Patna, Bihar 800005, India
Full list of author information is
available at the end of the article

Abstract

Gestation is a very significant phenomenon in predator-prey dynamics. It influences the future predation rates and the growth of species. Gestation is the period of development of an embryo or fetus in a female mammal, from conception to birth. It plays a critical role in population dynamics and reproductive strategies in ecological studies. This article presents a comparative study of eco-epidemic models with and without time delay terms. The model takes into account a prey-predator system, dividing the prey population into susceptible and infected compartments. This article incorporates a time delay into the predator growth term to represent gestation delay. This article investigates the impact of time delay as a gestation delay on the model's dynamics and compares the results with those of the non-delay model. Our analytical and numerical studies reveal that the time delay stabilizes the model, exhibits switching behaviour, and leads to chaotic behaviour through periodic doubling. Moreover, the gestation delay destabilizes the model by causing Hopf bifurcations to emerge at multiple points. Our findings indicate that the delay model has richer dynamics than the non-delay model. The numerical simulations using MATLAB, along with the DDE-biftool and Matcont packages, illustrate the bifurcation analysis, phase portraits, and time series plots for both models. Our findings highlight the significant effects of gestation delay on the dynamics of eco-epidemic models.

Keywords: Eco-epidemic predator-prey model; Stability analysis; Hopf bifurcation; Gestation Delay; Switching behaviour; Chaos

1 Introduction

In recent years, there has been a significant increase in the study of eco-epidemiological models as scientists strive to understand the intricate relationships between ecological and epidemiological processes. These models investigate the interspecies relationship and transmission of infectious diseases by combining ecological dynamics, such as predator-prey relationships, with epidemic dynamics. Time delays, representing the temporal lag in population responses to shifting environmental factors or disease dynamics, add a new

© The Author(s) 2025. **Open Access** This article is licensed under a Creative Commons Attribution-NonCommercial-NoDerivatives 4.0 International License, which permits any non-commercial use, sharing, distribution and reproduction in any medium or format, as long as you give appropriate credit to the original author(s) and the source, provide a link to the Creative Commons licence, and indicate if you modified the licensed material. You do not have permission under this licence to share adapted material derived from this article or parts of it. The images or other third party material in this article are included in the article's Creative Commons licence, unless indicated otherwise in a credit line to the material. If material is not included in the article's Creative Commons licence and your intended use is not permitted by statutory regulation or exceeds the permitted use, you will need to obtain permission directly from the copyright holder. To view a copy of this licence, visit <http://creativecommons.org/licenses/by-nc-nd/4.0/>.

dimension to these models. The use of mathematical models is crucial for comprehending the mechanisms behind species persistence and extinction. Theoretical biologists, physicists, and mathematicians extensively studied the dynamics of ecological models and provided important insights about complex biological processes [1]. Ecology has a rich historical background in studying predator-prey interactions, which continues to be a highly captivating research area for scientists worldwide. The eco-epidemiological systems field focuses on examining ecological systems, while considering the influence of epidemiological issues. Anderson and May [2] were the pioneering researchers who integrated ecological and epidemiological systems. Chattopadhyay and Arino are credited with coining the term “eco-epidemiology” to describe these systems [9]. Within the natural realm, individual species do not exist in isolation; rather, they engage in competitive interactions with other species present in their environment, struggling for resources such as habitat, sustenance, and opportunities for predation. Investigating parasites’ impact on biodiversity and ecosystem dynamics is a significant concern in conservation biology. It is important to find the threshold between populations staying alive and going extinct in systems with two or more species interacting and parasitism acting on them [13, 47]. Researchers have looked at the eco-epidemic predator-prey model and thought about infected prey where they are not considered any type of time delay term in their model [3, 9, 24, 33–35, 37, 41]. The researchers also considered predator diseases and studied them in their paper without incorporating a time delay term [11, 25, 42]. As we know, many ecological and biological phenomena are not instantaneous; they take time to unfold. These processes depend not only on the present state but also on past conditions. Therefore, such processes cannot be accurately described solely using ordinary differential equations (ODEs); instead, delay differential equations (DDEs) should be employed for more precise results. While ODEs only account for instantaneous changes, DDEs take into consideration the system’s past history, for example, maturation delay, reforestation, incubation delay, and gestation delay. Maturation delay refers to the time it takes for an animal to reach sexual maturity and reproductive capability. This delay varies significantly among different species, including lions, tigers, and dogs. A brief overview of the maturation delays for these animals: Female lions typically reach sexual maturity around 2 to 3 years of age, while males may take longer, generally maturing between 3 to 4 years. Female lions can breed every 2 to 3 years, with a gestation period of about 110 days [36]. The age at which dogs reach sexual maturity varies widely by breed. Smaller breeds may mature as early as 6 months, while larger breeds can take up to 18 to 24 months [10, 14]. Maturation delay in humans refers to the period it takes for an individual to reach full physical, sexual, and psychological maturity. Most girls reach their full adult height by around ages 16 to 18, while boys may continue to grow until about ages 18 to 21. Many researchers studied the impact of time delay and discovered that it had much richer dynamics than the non-delay model. The researchers have studied the ecological and biological model with time delay [5, 7, 29, 31, 38]. The time delay effect in the single-species model was studied, and it was found that the system has chaotic behaviour [22]. The prey-predator model with maturation delay has been studied [4, 12, 32]. The phenomenon of time delay has a significant influence on a system’s dynamics. Several eco-epidemiological models have been created and studied. Some of them include parts that happen over time delays [13, 16, 21, 26]. These articles studied the impact of time delay and found that the models have become chaotic about the delay parameter. The articles discuss the impact of incubation delay on predator-prey models

[19, 21, 28, 39]. Recent research in 2024 has focused on modelling infection spreading in tissue using a delay reaction-diffusion system [20]. The researchers have examined the multiple time delay models [15]. The researchers looked at the gestation delay model with prey refuge and found that Hopf bifurcation happens because of gestation delay [27]. In ecology modelling, gestation delay refers to the time lag between when a predator consumes its prey and when the predator gives birth to its offspring. Eco-epidemic models often incorporate this delay to reflect that predators do not immediately reproduce after consuming their prey. Gestation periods vary significantly across species, influenced by factors like size and reproductive strategies. For example, elephants have the longest gestation, lasting 18 to 22 months, while the Virginian opossum has one of the shortest at about 12 days. Other mammals, like Rhesus monkeys, have a gestation period of approximately 164 days and baboons around 187 days. Few researchers have studied the gestation delay in eco-epidemic models where infection is present in prey [18, 40, 44]. The researchers [44] looked at how gestation delay affected the dynamics of an eco-epidemic model with prey infection. In 2018, the researchers [46] looked into the complicated dynamics caused by gestation delay in Gause-type competition models. The model's findings show that the gestation delay causes Hopf bifurcation and switching properties. The study focussed on the effects of incubation and gestation periods in a prey-predator model with infection in prey [6]. The article [27] studied the impact of delay-induced eco-epidemiological models with a prey refuge. Their findings suggest that the gestation delay can destabilize the system due to the appearance of a Hopf bifurcation.

This article explores the impact of time delay, represented as τ , on an eco-epidemic model, particularly in the context of a SIP (susceptible-infected-predator) compartmental model, where (S) represents susceptible prey, (I) represents infected prey, and (P) represents predator. In this model, the disease can spread between prey populations and the predator preys on both susceptible and infected prey. However, the predation process involves a delay term, which represents a gestation delay.

Research objective of this article: The objective of this study is to investigate and compare the dynamics of an eco-epidemic model with and without a time delay, specifically focusing on the effects of gestation delay in the predator growth term on the stability and behaviour of the model. The study aims to analyze how the inclusion of time delay influences the model's dynamics, including the emergence of chaotic behaviour, switching dynamics, and Hopf bifurcations, thereby demonstrating that the delay model exhibits richer and more complex behaviours than the non-delay model. How does gestation delay impact stable equilibrium and unstable equilibrium?

Section 1 of the article provides an overview of previous research on eco-epidemiology modelling and its delayed effects. The proposed model is constructed in Sect. 2, while Sects. 3 and 4 examine the theoretical studies, including positivity, boundedness, equilibrium analysis, stability, and Hopf-bifurcation for the model with $\tau = 0$. Section 2.1 delves into the stability and bifurcation of the delay model, while Sect. 5 presents the numerical simulations for both models (Model (6)) and the delay model (Model (8)). The results and discussions are presented in Sect. 6, and the article concludes with a summary of the key findings in Sect. 7. The article aims to provide a comprehensive analysis of the eco-epidemic model, taking into account the time delay and its implications for the predator's reproduction rate. By examining the stability, bifurcation, and numerical simu-

lations of the model, the study offers valuable insights into the complex dynamics of eco-epidemiology.

2 Model formulation

Let the total population of prey be represented by N , which can be further divided into two compartments: susceptible individuals, denoted by S , and infected individuals, denoted by I . Additionally, consider the predator density, denoted by P . Assuming the absence of infected viruses, the prey population undergoes logistic growth. Therefore,

$$\frac{dN}{dt} = rN \left(1 - \frac{N}{k} \right). \quad (1)$$

Furthermore, we assume that reproduction is exclusive to susceptible prey, while infected prey lacks the ability to reproduce. Nevertheless, the infected prey still plays a role in influencing the growth of the susceptible prey towards reaching the carrying capacity k . Therefore,

$$\frac{dS}{dt} = rS \left(1 - \frac{S+I}{k} \right). \quad (2)$$

The predator, denoted as P , engages in predation on susceptible prey, exhibiting a Holling type-II functional response. Susceptible prey becomes infected upon contact with infected prey, and the transmission of infection follows the law of mass action with an infection rate denoted as L . Additionally, it is assumed that infected prey can recover, with the recovery process occurring at a rate of γ . Therefore,

$$\frac{dS}{dt} = rS \left(1 - \frac{S+I}{k} \right) - LSI - \frac{\alpha SP}{1+hS} + \gamma I. \quad (3)$$

The density of infected prey rises through interactions with susceptible prey, while recovering individuals contribute to a decrease in the infected prey density. Furthermore, infected prey experiences natural mortality at a rate, denoted as d . In this scenario, considering that the predator also engages in predation on infected prey, following a Holling type II functional response, the dynamics of the system can be described as follows;

$$\frac{dI}{dt} = LSI - t_r I - dI - \frac{\beta IP}{1+hI}. \quad (4)$$

The predation on susceptible and infected prey increases predator density, characterised by the Holling type II functional response with rates α_1 and β_1 , respectively.

$$\frac{dP}{dt} = \beta_1 \frac{PI}{1+hI} + \alpha_1 \frac{PS}{1+hS} - d_1 P. \quad (5)$$

By combining all the above assumptions, the model can be represented as follows:

$$\begin{aligned}
 \frac{dS}{dt} &= rS \left(1 - \frac{S+I}{K}\right) - LSI - \frac{\alpha SP}{1+hS} + \gamma I = Sf_1(S, I, P), \\
 \frac{dI}{dt} &= LSI - t_r I - dI - \frac{\beta IP}{1+hI} = If_2(S, I, P), \\
 \frac{dP}{dt} &= \beta_1 \frac{PI}{1+hI} + \alpha_1 \frac{PS}{1+hS} - d_1 P = Pf_3(S, I, P),
 \end{aligned}
 \tag{6}$$

where $S(0) \geq 0, I(0) \geq 0$, and $P(0) \geq 0$, respectively. Assume $\beta_1 = c\beta$ and $\alpha_1 = c_1\alpha$, where $c_1, c \in (0, 1)$ are conversation rate. All the parameters mentioned in Table 1 are taken as positive

2.1 Model (6) with delay term

To obtain more accurate results, we incorporated a gestation delay in the growth rate of the predator population in the model (6). Specifically, we modified the growth rate of the predator population to account for the gestation delay. The other assumptions of the model remained unchanged. The following equation describes the resulting growth of the predator population with gestation delay:

$$\frac{dP}{dt} = \beta_1 \frac{P(t-\tau)I(t-\tau)}{1+hI(t-\tau)} + \alpha_1 \frac{P(t-\tau)S(t-\tau)}{1+hS(t-\tau)} - d_1 P.
 \tag{7}$$

The model (6) with the gestation delay is as follows:

$$\begin{aligned}
 \frac{dS}{dt} &= rS \left(1 - \frac{S+I}{k}\right) - LSI - \frac{\alpha SP}{1+hS} + \gamma I, \\
 \frac{dI}{dt} &= LSI - t_r I - dI - \frac{\beta IP}{1+hI}, \\
 \frac{dP}{dt} &= \beta_1 \frac{P(t-\tau)I(t-\tau)}{1+hI(t-\tau)} + \alpha_1 \frac{P(t-\tau)S(t-\tau)}{1+hS(t-\tau)} - d_1 P,
 \end{aligned}
 \tag{8}$$

where the initial function is $\phi = (\phi_1, \phi_2, \phi_3)$, defined in the Banach space $C_+ = \{\phi \in C([-\tau, 0], R_+^3) : S(\xi) = \phi_1(\xi), I(\xi) = \phi_2(\xi), P(\xi) = \phi_3(\xi)\}$, where $\phi_i(\xi) \geq 0, \xi \in [-\tau, 0], \phi_i > 0, i = 1, 2, 3$ and $\phi = \{\phi_1, \phi_2, \phi_3\} \in C([-\tau, 0], R_+^3)$. Then the Banach space of all continuous function mapped from $[-\tau, 0] \rightarrow R_+^3$, where we define $R_+^3 = \{(S, I, P) : S \geq 0, I \geq 0, P \geq 0\}$. This initial condition is similar to the articles published by researchers [23, 45] If the value of $\tau = 0$, the model (8) can be categorized as a simple non-delay model (ODE model). On the other hand, in cases when $\tau \neq 0$, the model (8) is often denoted as a delay differential equation (DDE) model. All parameters are positive constant, and τ represents the gestation delay in the reproduction of the predator after consuming the prey (both susceptible and infected prey). The meaning of all other parameters is the same as in the model (6).

3 Theoretical studies for the model (6)

3.1 Positivity

Theorem 3.1 *The solutions of the given model (6) with initial value $S(0) \geq 0, I(0) \geq 0$ and $P_1(0) \geq 0$ are positive.*

Table 1 Parameters used in the model (6) and model (8)

Parameters	
r	Intrinsic growth rate of susceptible prey
k	Carrying capacity of prey
L	Disease transmission rate
α	Attack rate of predator on susceptible prey
β	Attack rate of predator on infected prey
d	Death rate of infected prey
t_r	Treatment rate
d_1	Death rate of predator
β_1	conversion rate of Infected prey into predator biomass
h	Handling time
γ	Recovery rate.

Proof Since the function $Sf_1(S, I, P)$, $If_2(S, I, P)$, and $Pf_3(S, I, P)$ are taken from right side of model (6) are continuous function and locally Lipschitzian on R^3_+ , implies that the solution $(S(t), I(t), P(t))$ exists and is unique on $[0, \epsilon]$, where $0 < \epsilon < \infty$ [17]. For the positive integrating model (6), with respect to the initial condition, we get the solution as follows;

$$S(t) = S(0)e^{\int_0^t f_1(S(s), I(s), P(s)) ds} \geq 0,$$

$$I(t) = I(0)e^{\int_0^t f_2(S(s), I(s), P(s)) ds} \geq 0,$$

$$P(t) = P(0)e^{\int_0^t f_3(S(s), I(s), P(s)) ds} \geq 0,$$

where $S(0) \geq 0, I(0) \geq 0$, and $P(0) \geq 0$. Hence, all the solutions of the model (6) are positive. □

3.2 Boundedness of the solution

Theorem 3.2 *In R^3_+ , all the solutions of the model (6) are uniformly bounded.*

Proof let us assume $Z = S + I + P$, by differentiate it we get;

$$\frac{dZ}{dt} = \frac{dS}{dt} + \frac{dI}{dt} + \frac{dP}{dt}, \tag{9}$$

taking the value of $\frac{dS}{dt}, \frac{dI}{dt}$ and $\frac{dP}{dt}$ from model (6), we have,

$$\begin{aligned} \frac{dZ}{dt} &= rS \left(1 - \frac{S+I}{k} \right) - LSI - \frac{\alpha SP}{1+hS} + \gamma * I + LSI - trI - dI - \frac{\alpha IP}{1+hI} \\ &\quad + \beta_1 \frac{PI}{1+h_1I} + \alpha_1 \frac{PS}{1+hS} - d_1P. \\ \frac{dZ}{dt} + \mu p &= S \left[r \left(1 - \frac{S+I}{k} \right) + \mu \right] - I(d + tr - \mu) - P(d_1 - \mu) \\ &\leq \left(\frac{k(r + \mu)^2}{2r} \right) = \phi. \end{aligned}$$

If $\phi > \min(d + tr, d_1)$ and using upper bound $(1 + \mu)$, we define $\phi > 0$ such that

$$\frac{dZ}{dt} + \mu p \leq \phi, \quad \forall t \in (0, t_b)$$

with the theory of differential inequality (Grönwall’s inequality) [8], we obtain

$$0 < p(x, y, I_1) \leq \frac{\phi}{\mu}(1 - e^{-\mu t}) + Z(S(0), I(0), P(0))e^{-\mu t}.$$

We have $0 < Z < \frac{\phi}{\mu}$ for $t \rightarrow \infty$. Hence, it is clear that all solutions to the system will remain in the region

$$\tau = \{(S, I, P) \in R_+^3 : Z \leq \frac{\phi}{\mu}\} \text{ for all time.} \quad \square$$

3.3 Equilibrium analysis

By solving the equation $\frac{dS}{dt} = 0, \frac{dI}{dt} = 0$ and $\frac{dP}{dt} = 0$ simultaneously we get the following equilibrium point. (i) Trivial equilibrium $E_0 = (0, 0, 0)$ always exists for the model. (ii) One disease and predator-free equilibrium $E_1 = (k, 0, 0)$ exist. (iii) Disease-free equilibrium $E_2 = (S^*, 0, P^*)$, where $S^* = \frac{d_1}{\alpha_1 - hd_1}$ and $P^* = \frac{r}{\alpha} \left(1 - \frac{S^*}{k}\right) \left(\frac{d_1}{\alpha_1 - hd_1}\right)$ provided $k\beta > hd_1k + d_1$, Predator-free equilibrium $E_3 = (S^*, I^*, 0)$, $S^* = \frac{d+t_r}{L}$ and $I^* = \frac{r(k-S^*)}{r+Lk-\gamma k}$. Interior equilibrium point $E_4 = (S^*, I^*, P^*)$, where $S^* = \frac{d_1+I^*(d_1h-\beta_1)}{(\alpha_1-d_1h+I^*(\alpha_1h\beta h-d_1h^2))}$, $P^* = \frac{B}{\beta(\alpha_1-d_1h+I^*(\alpha_1h\beta h-d_1h^2))}$, $B = L\{d_1(1+hI^*)-\beta_1I^*\}(1_hI^*)-(t_r+d)(1+hI^*)\{\alpha_1(1+hI^*)+\beta_1I^*h-d_1h(1+hI^*)\}$ and I^* calculated from the equation

$$r(k - S^*)(1 + hS^*) - LI^*k - \alpha P^* + \gamma I^* = 0. \tag{10}$$

From Equation (10), we have only one I^* as $I^* = \frac{r(k-S^*)(1+hS^*)-\alpha P^*}{Lk-\gamma}$.

4 Local stability of model (6)

For local stability, first linearise the nonlinear system about the equilibrium, find the Jacobian matrix, and calculate the eigenvalue. The eigenvalue of the Jacobian matrix indicates stability. If all the eigenvalues values have a negative real part, then that equilibrium point is asymptotically stable, [30]. So, the Jacobian matrix of the linearised system is as follows;

$$J = \begin{bmatrix} A_1 & A_2 & A_3 \\ A_4 & A_5 & A_6 \\ A_7 & A_8 & A_9 \end{bmatrix}, \tag{11}$$

where $A_1 = r - \frac{2S^*}{k} - LI^* - \frac{\alpha P^*}{(1+hS^*)^2}$, $A_2 = -\frac{S^*}{k} - LS^* + \gamma$, $A_3 = \frac{\alpha S^*}{(1+hS^*)}$, $A_4 = LI^*$, $A_5 = LS^* - tr - d - \frac{\beta P^*}{(1+hI^*)^2}$, $A_6 = \frac{\alpha I^*}{(1+hI^*)}$, $A_7 = \frac{\alpha_1 P^*}{(1+h_1S^*)^2}$, $A_8 = \frac{\beta_1 P^*}{(1+hI^*)^2}$, $A_9 = \frac{\beta_1 I^*}{(1+hI^*)} + \frac{\alpha_1 S^*}{(1+hS^*)} - d_2$. Jacobian matrix at trivial equilibrium as follows:

$$J_0 = \begin{bmatrix} r & 0 & 0 \\ 0 & -d & 0 \\ 0 & 0 & -d_1 \end{bmatrix} \tag{12}$$

Here eigenvalues are $r, -d, -d_1$ so equilibrium point is unstable.

Theorem 4.1 *The equilibrium point $(k, 0, 0)$ is asymptotically stable if $r < 2$ and $d_1 > \frac{\alpha k}{1+h_1k}$*

Proof Jacobian matrix of $(K,0,0)$;

$$J_1 = \begin{bmatrix} r-2 & Lk & \frac{\alpha k}{1+hk} \\ 0 & -tr-d & 0 \\ 0 & 0 & \frac{\alpha k}{1+hk} - d_1 \end{bmatrix} \tag{13}$$

In the above matrix, we can easily see that all the eigenvalues of the matrix are negative if $r < 2$ and $\frac{\alpha k}{1+hk} < d_1$. Hence, the equilibrium point $(k,0,0)$ is asymptotically stable. \square

Theorem 4.2 *Diseases-free and interior equilibrium are asymptotically stable if they follow the Routh–Hurwitz criterion.*

Proof The theorem follows from Routh–Hurwitz, so the proof is omitted. \square

4.1 Hopf bifurcation analysis

Theorem 4.3 *Hopf bifurcation for the interior $E(S^*, I^*, P^*)$ appear when the carrying capacity attains $r = r^{hb}$ in the domain $D_{hb} = r^{[hb]}$*

$$D_{hb} = \{r^{[hb]} \in \mathbb{R}^+ : H(k^{[hb]}) \\ [c_1(r)c_2(r) - c_3(r)]_{r=r^{[hb]}} = 0 \text{ with.} \\ a_2(r^{[hb]}) > 0, \left[\frac{dH(k)}{dr} \right]_{r=r^{[hb]}} \neq 0 \}.$$

Proof The characteristic equation of J_* is

$$\lambda^3 + c_1\lambda^2 + c_2\lambda + c_3 = 0, \tag{14}$$

where $c_1, c_2,$ and c_3 are mentioned in equation (14), by differentiating characteristic equation (14), we have

$$\frac{d\lambda}{d\theta} = \frac{-(\lambda^2\dot{c}_1 + \lambda\dot{c}_2 + \dot{c}_3)}{3\lambda^2 + 2c_1\lambda + c_2}. \tag{15}$$

Put $\lambda = i\sqrt{c_2}$ in (15), we have

$$\frac{d\lambda}{dk} = \frac{\dot{c}_3 - c_2\dot{c}_1 + i\dot{c}_2\sqrt{c_2}}{2(c_2 - ic_1\sqrt{c_2})}.$$

After rationalization, we have

$$\begin{aligned} \frac{d\lambda}{dk} &= \frac{\dot{c}_3 - (c_2\dot{c}_1 + c_2\dot{c}_1)}{2(c_1^2 + c_2)} + \frac{(i\sqrt{c_2}(c_1\dot{c}_3 + c_2\dot{c}_2 - c_1c_2\dot{c}_1)}{2c_2(c_1^2 + c_2)} \\ &= -\frac{-\frac{dH}{dk}}{2(c_1^2 + c_2)} + i \left[\frac{\sqrt{c_2}\dot{c}_2}{2c_2} - \frac{c_1\sqrt{c_2}\frac{dH}{dk}}{2c_2(c_1^2 + c_2)} \right]. \end{aligned}$$

Here, $\left[\frac{d\text{Re}(\lambda)}{dr} \right] = \frac{-\frac{dH}{dr}}{2(a_1^2+a_2)} \neq 0$, by monotonicity restriction in the real part of the complex root $\left[\frac{dR(\lambda)}{dr} \right] \neq 0$ [25, 43], the transversality condition $\frac{dH}{dr} \neq 0$ ensure the existence of Hopf bifurcation. \square

4.2 Theoretical study of model (8)

This section studied the theoretical aspects of the model (8), in which the positivity of the model and the stability of the solution about the interior equilibrium have been investigated. Additionally, the Hopf bifurcation about τ was studied. The equilibrium analysis of the model (8) is the same as that of the model (6).

4.2.1 Positivity of the delay model (8)

For the biological significance, we need to demonstrate that the model we constructed has a positive solution. The positivity of the solution implies the survival of the population. To show positivity, follow the method of Yang et al. [45].

Theorem 4.4 *All solutions of model (8) with the with initial value $S(0) \geq 0, I(0) \geq 0$ and $P_1(0) \geq 0$ are positive.*

Proof The proof is similar to that presented in paper [26]. By integrating the equations of the model (8) separately, we have:

$$S(t) = S(0)e^{\int_0^t \left(r \left(1 - \frac{S(\theta)+I(\theta)}{K} \right) - LI(\theta) - \frac{\alpha P(\theta)}{1+hS(\theta)} + \gamma I(\theta) \right) d\theta} \geq 0. \tag{16}$$

This implies that $S(t) > 0$ for all t whenever $S(0) \geq 0$. Similarly, $I(t) \geq 0$ for all t whenever $I(0) > 0$. Now, from the last equation of the model (8),

$$\frac{dP}{dt} = \beta_1 \frac{P(t-\tau)I(t-\tau)}{1+h_1I(t-\tau)} + \alpha_1 \frac{P(t-\tau)S(t-\tau)}{1+hS(t-\tau)} - d_1P, \tag{17}$$

by dividing both sides of this equation by P and integrating, we obtain:

$$P(t) = P(0)e^{\int_0^t \left(\beta_1 \frac{P(\theta-\tau)I(\theta-\tau)}{1+h_1I(\theta-\tau)} + \alpha_1 \frac{P(\theta-\tau)S(\theta-\tau)}{1+hS(\theta-\tau)} - d_1P(\theta) \right) d\theta} \geq 0. \tag{18}$$

Thus, $P(t) > 0$ for all t whenever $P(0) > 0$. Hence, all the solutions of model (8) are positive. □

4.2.2 Stability and bifurcation

To study the local stability and bifurcation of the model (8) around point E_4 , we need to linearise the model and find the Jacobian matrix around that point.

$$\frac{dX}{dt} = \begin{bmatrix} A_1 & A_2 & A_3 \\ A_4 & A_5 & A_6 \\ k_3 & A_7 & k_4 \end{bmatrix} X(t) + \begin{bmatrix} 0 & 0 & 0 \\ 0 & 0 & 0 \\ k_1 & 0 & k_2 \end{bmatrix} X(t-\tau), \tag{19}$$

where $K_3 = 0, k_1 = \frac{\alpha_1 P}{(1+hS)^2}, k_2 = \frac{\alpha_1 S}{(1+hS)}, k_4 = -d_1 + \frac{\beta_1 \gamma}{1+h\gamma}$ and other elements are same as defined in (11). The required characteristic equation of the matrix (19) $Det(\lambda I - A - B e^{-\lambda \tau})$ as follows:

$$\lambda^3 + a_1 \lambda^2 + a_2 \lambda + a_3 + e^{-\lambda \tau} (b_1 \lambda^2 + b_2 \lambda + b_3) = 0, \tag{20}$$

where $a_1 = -k_4 - A_5 - A_1$, $a_2 = k_4A_5 - A_1A_5 + A_1A_5 - A_2A_4$, $a_3 = A_1A_5k_4 + A_2A_4k_4 - A_3A_4k_2$, $b_1 = -k_3$, $b_2 = -A_1k_3 + A_5k_3 - A_6k_2 - k_1A_3$, $b_3 = -A_1A_5k_3 + A_1A_6k_2 + A_2A_4k_3 - A_2A_6k_1 - A_3A_4k_2 + k_1A_5A_3$.

Equation (20) has infinitely many roots $\tau > 0$. By putting $\lambda = iw (w > 0)$ in the equation (20), we have

$$(a_1w^2 - w^3) = (b_3 - b_1w^2)\cos(w\tau) + b_2w\sin(w\tau), \tag{21a}$$

$$w^3 - a_2w = b_2w\cos(w\tau) - (b_3 - b_1w^2)\sin(w\tau). \tag{21b}$$

From equation (21a–21b), we can write the above system of equations as,

$$\cos(\omega\tau) = \frac{(a_1\omega^2 - a_3)(b_3 - b_1\omega^2) + (\omega^3 - a_2\omega)b_2\omega}{(b_3 - b_1\omega^2)^2 + b_2^2\omega^2}, \tag{22a}$$

$$\sin(\omega\tau) = \frac{b_2w(a_1w^2 - a_3) - (w^3 - a_2w)(b_3 - b_1w^2)}{(b_3 - b_1w^2)^2 + b_2^2w^2}. \tag{22b}$$

The critical value of time delay under the condition $b_2w(a_1w^2 - a_3) - (w^3 - a_2w)(b_3 - b_1w^2) > 0$

$$\tau_k^j = \frac{2\pi j}{\omega_k} + \frac{1}{\omega_k} \arcsin \left(\frac{b_2w(a_1w^2 - a_3) - (w^3 - a_2w)(b_3 - b_1w^2)}{(b_3 - b_1w^2)^2 + b_2^2w^2} \right) \tag{23}$$

and if $b_2w(a_1w^2 - a_3) - (w^3 - a_2w)(b_3 - b_1w^2) < 0$, then

$$\tau_k^j = \frac{2\pi j}{\omega_k} + \frac{2\pi}{\omega} - \frac{1}{\omega_k} \arcsin \left(\frac{b_2w(a_1w^2 - a_3) - (w^3 - a_2w)(b_3 - b_1w^2)}{(b_3 - b_1w^2)^2 + b_2^2w^2} \right), \tag{24}$$

where $k = 1, 2, 3, j = 0, 1, 2, \dots$, and $\tau_0 = \min_{k=1,2,3} \tau_k^0$. After squaring and adding them, we have,

$$w^6 + (a_1^2 - b_1^2 - 2a_2)w^4 + (a_2^2 - 2a_1a_3 + 2b_1b_3 - b_2^2)w^2 + (a_3^2 - b_3^2) = 0. \tag{25}$$

Putting $w^2 = \epsilon$, we have

$$h(\epsilon) = \epsilon^3 + c_1\epsilon^2 + c_2\epsilon + c_3, \tag{26}$$

where $c_1 = a_1^2 - b_1^2 - 2a_2$, $c_2 = a_2^2 - 2a_1a_3 + 2b_1b_3 - b_2^2$, $c_3 = a_3^2 - b_3^2$.

The equation (26) has at least one positive if $c_1 > 0, c_3 > 0$ by Descartes' rule of sign.

Lemma 4.5 *If $\tau = \tau_1$ and $h'_1(w^2) \neq 0$, the equation (20) has a pair of purely imaginary roots $\pm iw$ and $\frac{d(\text{Real}(\lambda(\tau)))}{d\tau} \Big|_{\tau_1} \neq 0$*

Proof Let us assume $f_1(\lambda) = \lambda^3 + a_1\lambda^2 + a_2\lambda + a_3$ and $g(\lambda) = b_1\lambda^2 + b_2\lambda + b_3$, the equation (20) be written as the form;

$$f(\lambda) + g(\lambda)e^{-\lambda\tau} = 0 \tag{27}$$

put $\lambda = iw$ into equation (27), we get

$$f(iw) + g(iw)(\cos(iw) - \sin(iw)) = 0 \tag{28}$$

Thus, we have

$$\frac{f(iw) + \bar{f}(iw)}{2} = -\frac{g(iw) + \bar{g}(iw)}{2} \cos(w\tau) + i \frac{g(iw) - \bar{g}(iw)}{2} \sin(iw)$$

$$\frac{f(iw) - \bar{f}(iw)}{2} = \frac{g(iw) - \bar{g}(iw)}{2} \cos(w\tau) + i \frac{g(iw) + \bar{g}(iw)}{2} \sin(iw)$$

Then we get

$$f(iw)\bar{f}(iw) - g(iw)\bar{g}(iw) = 0 \tag{29}$$

Using Equation (26), we have

$$h(w^2) = f(iw)\bar{f}(iw) - g(iw)\bar{g}(iw) = 0. \tag{30}$$

Next, assume that $\lambda = iw$ is not a purely imaginary roots of Eq. (20), differentiating Eq. (27) with respect to $\lambda = iw$, we get

$$f'(iw) + g'(iw)e^{-iw\tau} - \tau g(iw)e^{-iw\tau}. \tag{31}$$

Using equation (27), we write

$$f(iw) + g(iw)e^{-iw\tau}. \tag{32}$$

Solving equation (31) and using equation (32) and (29), we get

$$\begin{aligned} \tau_1 &= \frac{g'(iw)}{g(iw)} - \frac{f'(iw)}{f(iw)} \\ &= \frac{g'(iw)\bar{g}(iw) - f'(iw)\bar{f}(iw)}{f(iw)\bar{f}(iw)}. \end{aligned}$$

It is easy to show that

$$\begin{aligned} \text{Im}\tau_1 &= \text{Im} \frac{g'(iw)\bar{g}(iw) - f'(iw)\bar{f}(iw)}{f(iw)\bar{f}(iw)} \\ &= -i \frac{g'(iw)\bar{g}(iw) - f'(iw)\bar{f}(iw)}{2f(iw)\bar{f}(iw)} - \frac{f'(iw)\bar{f}(iw) - g'(iw)\bar{g}(iw)}{2f(iw)\bar{f}(iw)}. \end{aligned}$$

Differentiating equation (30) w.r.t w , we have

$$2wh'(w^2) = if'(iw)\bar{f}(iw) - i\bar{f}(iw)f(iw) - ig'(iw)\bar{g}(iw) + i\bar{g}(iw)g(iw). \tag{33}$$

So,

$$\text{Im}\tau_1 = \frac{wh'(w^2)}{f(iw)f(iw)}.$$

Thus $h'(iw^2) \neq 0$ indicates that $\text{Im } \tau_1 \neq 0$, which contradicts that imaginary of τ is zero. Hence, $\lambda = iw$ is purely the imaginary root of Equation (20).

Now we move to show transversality condition in the other part of the lemma. Differentiating equation (27) over τ , we get

$$f'(\lambda)\frac{d\lambda}{d\tau} + g'(\lambda)e^{-\lambda\tau}\frac{d\lambda}{d\tau} - \tau g(\lambda)e^{-\lambda\tau}\frac{d\lambda}{d\tau} - \lambda g(\lambda)e^{-\lambda\tau} = 0 \tag{34}$$

After simplifying, we get

$$\begin{aligned} \left.\frac{d\lambda(\tau)}{d\tau}\right|_{\tau_1} &= \frac{\lambda g(\lambda)e^{-\lambda\tau}}{g'(\lambda)e^{-\lambda\tau} + f'(\lambda) - \tau g(\lambda)e^{-\lambda\tau}} \\ &= \frac{\lambda g(\lambda)e^{-\lambda\tau} [g'(\lambda)e^{-\lambda\tau} + f'(\lambda) - \tau g(\lambda)e^{-\lambda\tau}]}{[g'(\lambda)e^{-\lambda\tau} + f'(\lambda) - \tau g(\lambda)e^{-\lambda\tau}]^2} \\ &= \frac{\lambda [g(\lambda)\bar{g}'(\lambda) + f'(\lambda) - \tau \bar{g}^2(\lambda)]}{[g'(\lambda)e^{-\lambda\tau} + \bar{f}'(\lambda)f(\lambda) - \tau g(\lambda)e^{-\lambda\tau}]^2}. \end{aligned}$$

Obviously, we have

$$\begin{aligned} \frac{d(\text{Re}\lambda(\tau))}{d\tau} &= \frac{\text{Re}\lambda [g(\lambda)\bar{g}'(\lambda) + f'(\lambda) - \tau \bar{g}^2(\lambda)^2] - \bar{\lambda} [g'(\lambda)g(\lambda) - f'(\lambda)\bar{f}'(\lambda) - \tau \bar{g}^2(\lambda)]}{2[g'(\lambda)e^{-\lambda\tau} + \bar{f}'(\lambda)f(\lambda) - \tau g(\lambda)e^{-\lambda\tau}]^2} \Big|_{\tau_1} \\ &= \frac{w^2 h'(w^2)}{[g'(\lambda)e^{-\lambda\tau} + \bar{f}'(\lambda)f(\lambda) - \tau g(\lambda)e^{-\lambda\tau}]^2} \neq 0. \end{aligned}$$

It is clear that the sign of $\frac{d(\text{Re}\lambda)}{d\tau}$ depends on $w^2 h'(w^2)$. Proof completed. □

Now from Lemma 1, we can say that for $\tau = \tau^*$ and $h^*(w^*) \neq 0$ the Equation (20) has a pair of purely imaginary roots $\pm iw$ and $\frac{d(\text{Re}\lambda(\tau))}{d\tau} \neq 0$ at $\tau^* \neq 0$, Hence the important result on equilibrium point E_4 .

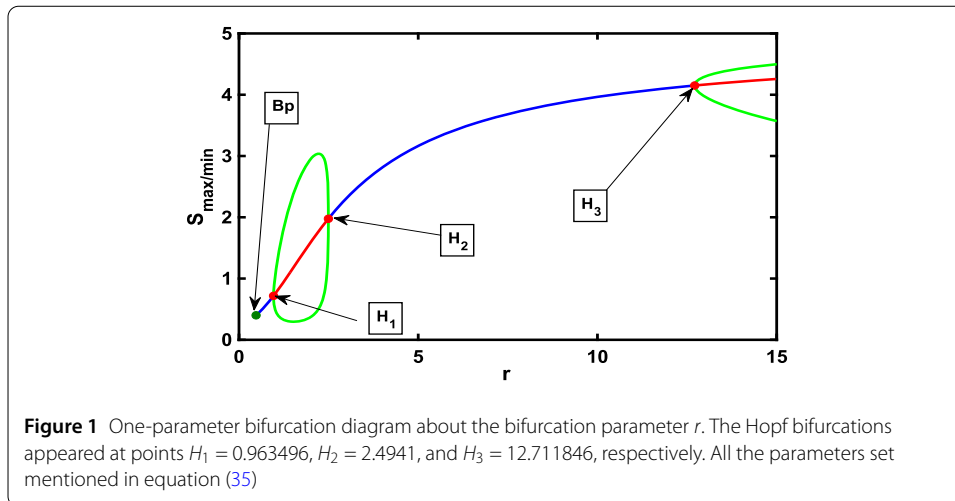
Theorem 4.6 *The interior equilibrium point E_4 is asymptotically stable for $\tau = 0$ if and only if the following conditions are satisfied: $a_1 > 0$, $a_3 > 0$, and $a_1 a_2 > a_3$. If $\tau \neq 0$ and $h'(w^2) \neq 0$, the system undergoes a Hopf bifurcation around E_4 .*

Proof The characteristic equation for $\tau = 0$ is obtained by putting $\tau = 0$ in Equation (20). By the Routh–Hurwitz criteria, we can conclude that if the conditions $a_1 > 0$, $a_3 > 0$, and $a_1 a_2 > a_3$ are satisfied, then the interior equilibrium is asymptotically stable. The proof of this part is omitted.

Now, we move on to the other part of the theorem. If $\tau \neq 0$ and $h'(w^2) \neq 0$, then the transversality condition $\frac{d(\text{Re}\lambda(\tau))}{d\tau} \neq 0$ at $\tau^* \neq 0$ is satisfied (see the proof in Lemma 4.5). Hence, the theorem is proved. □

5 Numerical simulation

This section encompasses numerical simulations of both the model without delay ($\tau = 0$) and with delay ($\tau \neq 0$). The delay model is tackled using MATLAB’s DDE solvers, while



ODE solvers like ode45 are employed for the non-delay model. Bifurcation analysis of the model is conducted using Matcont for the non-delay scenario and DDE Biftool for the delay case in MATLAB.

For the entire numerical simulation, we set the following fixed parameters, as mentioned:

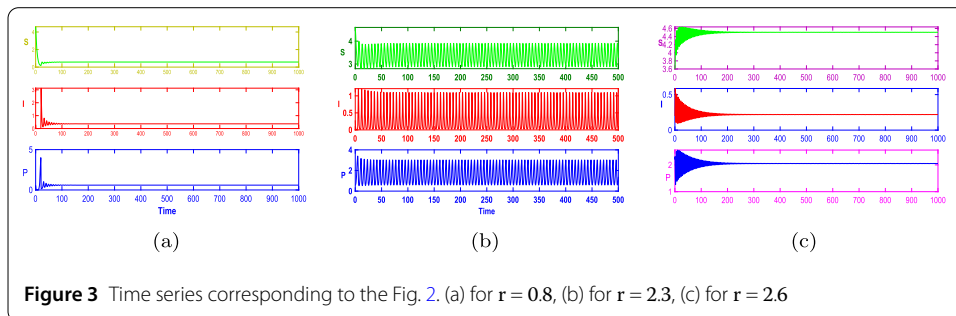
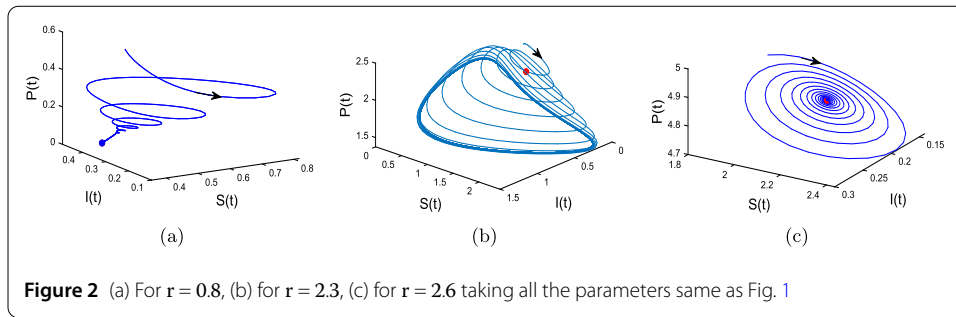
$$\begin{aligned}
 k = 5, \alpha = 0.5, \beta = 0.61, L = 1.5, h = 0.5, \alpha_1 = 0.1, \beta_1 = 0.5, \\
 tr = 0.5, \gamma = 0.2, d = 0.1, d_1 = 0.2.
 \end{aligned}
 \tag{35}$$

Now, let's first discuss the numerical simulation for the non-delay model, where $\tau = 0$. The bifurcation diagram in Fig. 1 illustrates the switching behaviour of the model as r is taken as the bifurcation parameter. Population oscillations or fluctuations are depicted through time series plotting.

5.1 Bifurcation diagram, time series and phase portraits for non-delayed model (6)

Figure 1 expresses the bifurcation about the parameter r , which describes three Hopf points: 0.963496, 2.4941, and 12.711846, respectively, around the interior equilibrium point. The interior equilibrium is stable for (i) $0.476 < r < 0.963496$, unstable in the region (ii) $0.9634 < r < 2.4941$, again stable in (iii) $2.4941 < r < 12.711846$, and lastly becomes unstable after 12.71184. The stable equilibrium loses its stability at Hopf points and emerges into a limit cycle. There is more than one Hopf point obtained in the region $0 < r < 20$; hence, it shows the switching behaviour of model (6). The limit cycle and periodic solution are obtained after the Hopf point in the unstable region, shown in Fig. 2 (b) and Fig. 3 (b), respectively.

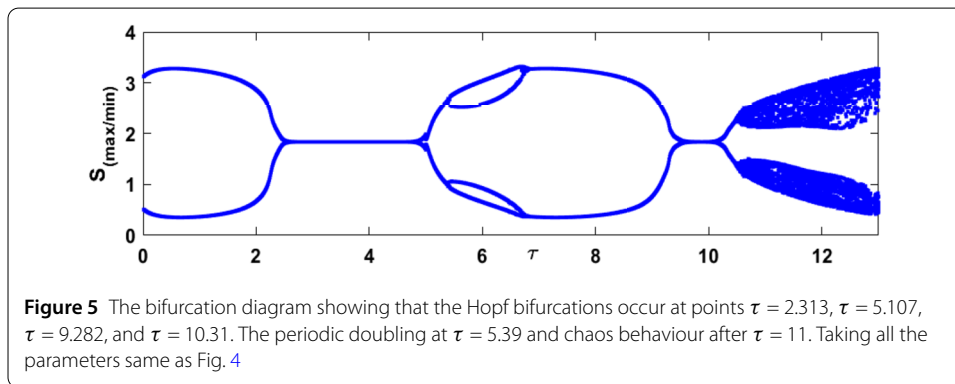
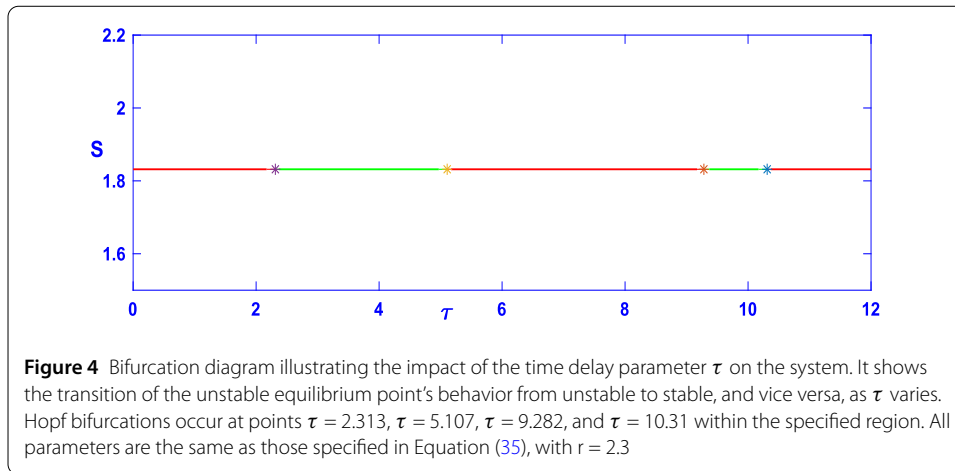
Figure 3 (a) demonstrates the absence of any oscillation or fluctuation in the population over a longer time frame. This observation suggests that the solution of model (6) regarding the interior equilibrium remains stable when $r = 0.8$. Figure 3 (b) demonstrates that all populations exhibit oscillatory motion, as shown by the periodic solution that represents the long-term behaviour of model (6). This indicates that the model referenced as (6) exhibits instability in relation to the inner equilibrium for $r = 2.3$. Similarly, the model



remains stable when $r = 2.6$, as seen in Fig. 3 (c). The model (6) demonstrates the phenomenon of switching behaviour with respect to the parameter r in the vicinity of the interior equilibrium. The model’s switching behaviour, as represented by (6), is seen in Fig. 1. The stability of model (6) undergoes a transition from stable to unstable and then back to stable via a Hopf bifurcation. This bifurcation is seen at three specific points: 0.963496, 2.4941, and 12.711846, respectively. There is no text provided.

5.2 Numerical simulation of the delay model with non-zero delay ($\tau \neq 0$)

The present subsection primarily examines the influence of the time delay parameter τ on the model (8) in two scenarios: stable and unstable equilibrium, with $\tau = 0$. To denote the occurrence of Hopf Bifurcation, Period Doubling (PD), and Chaos in a bifurcation diagram, use the following visual indicators: **Hopf Bifurcation**: In a bifurcation diagram, the existence of Hopf bifurcation may be identified by observing the following visual indicators: The Hopf bifurcation in a bifurcation diagram is defined by the appearance of a limit cycle originating from a fixed point when a parameter is altered. This transition happens when a pair of eigenvalues, which are complex conjugates, of the linearized system cross the imaginary axis, moving from the left half-plane to the right half-plane. A tiny amplitude oscillation, known as a limit cycle, may be seen visually in the bifurcation diagram. This oscillation emerges from a steady state, also known as a fixed point, and increases in amplitude when the parameter is adjusted. **Period Doubling (PD)**: PD in the bifurcation diagram is characterised by the abrupt appearance of a new branch or curve replicating the existing branch. The new branch has a period of twice as long as the previous one. In the plot of S_{max} against τ , the phenomenon known as PD is shown by a distinctive “fork” or “pitchfork” form. This shape indicates that the original branch divides into two new branches, as seen in Fig. 5. **Chaos**: Chaos is shown in the bifurcation diagram as a densely populated, seemingly haphazard, and unexpected arrangement of data points. Usually, chaos is preceded by a sequence of period-doubling bifurcations, resulting in an unlim-

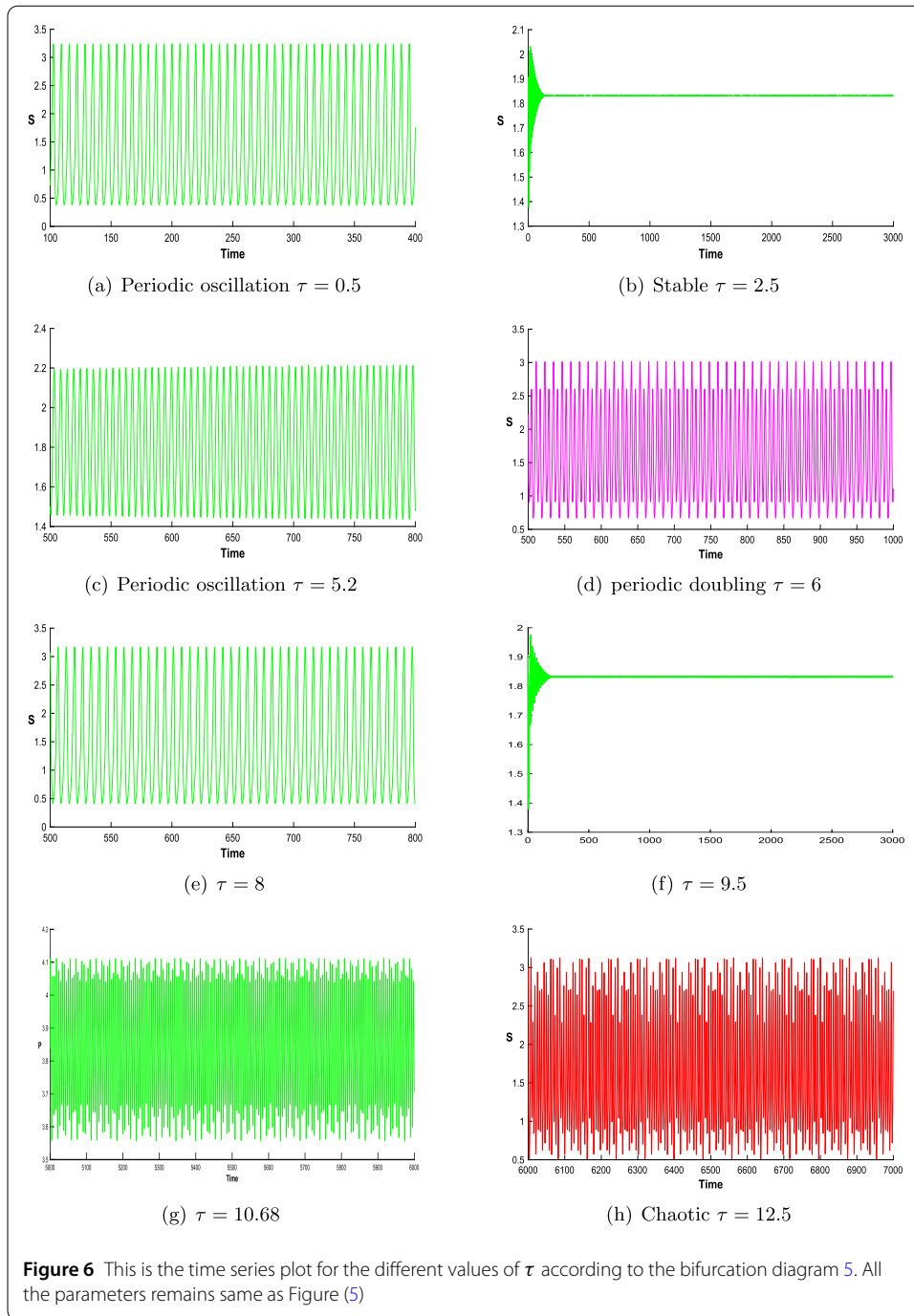


ited number of periodic orbits. In the S_{\max} versus τ parameter diagram, Chaos is represented as a cluster or band of points that seem to be scattered randomly. Given the fixed parameters described in Equation (35) and the starting circumstances (1.981, 0.223, 5.32), we can conclude that a stable interior equilibrium point E occurs when r is equal to 2.6. As the value of τ grows, the stability of E undergoes a shift, characterised by a switching behaviour (Fig. 8). The internal equilibrium, which is not stable, exhibits switching behaviour (Fig. 5). It becomes stable via Hopf bifurcation, loses stability, and shows periodic doubling and chaos. The system experiences Hopf bifurcations at $\tau = 5.107$, $\tau = 9.282$, and $\tau = 10.31$, resulting in the emergence of periodic and chaotic solutions.

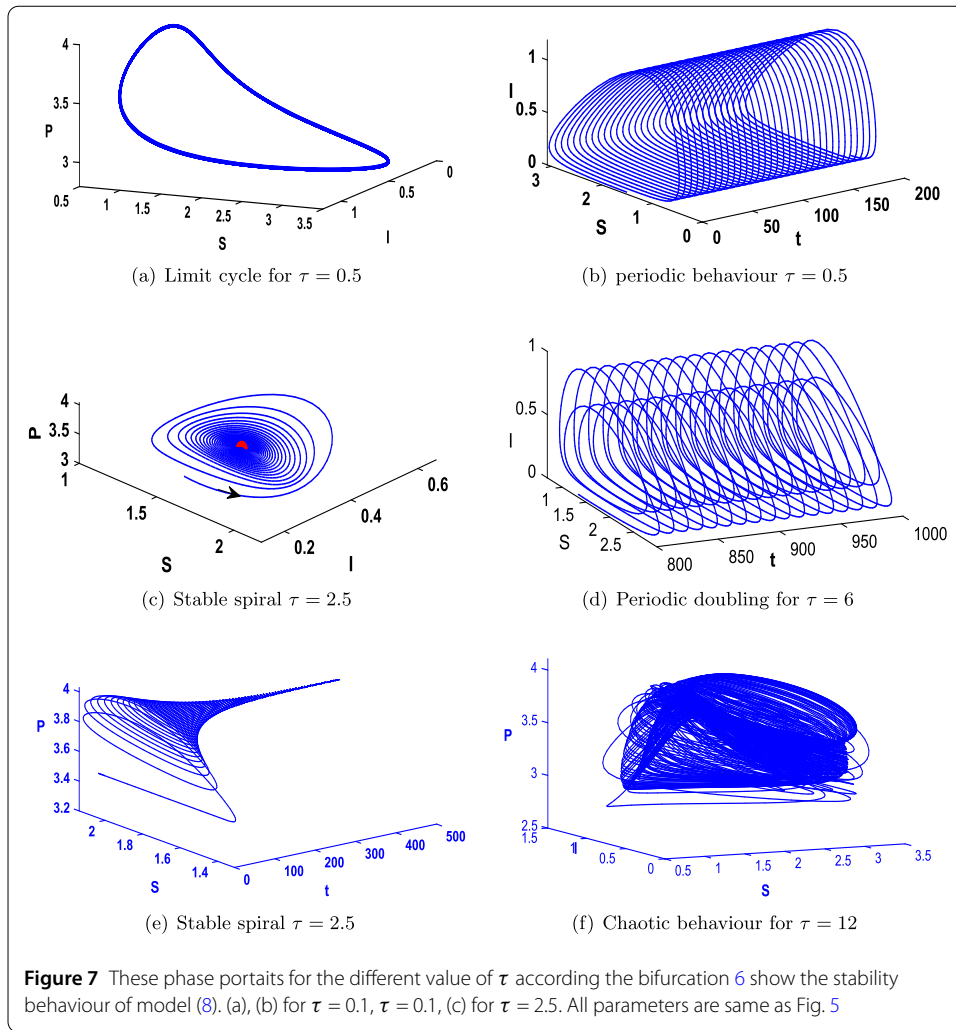
5.2.1 Impact of time delay on the model for the unstable equilibrium

This section shows the impact of the time delay on the model (8) for the unstable interior equilibrium for $\tau = 0$. Figure 4 bifurcation diagram about the parameter τ and Fig. 5 bifurcation diagram $S_{\max/\min}$ vs τ .

In Fig. 6 (a), (c), and (e), respectively, periodic oscillations are shown. Figure 6 (b) and (f) show that the solution of the model (8) is stable, as there are zero amplitudes, which means no fluctuations in the solution for a long time. Figure 6 (d) shows that the solution of the model (8) exists in periodic doubling, with two types of periods obtained. The chaotic behaviour of the model (8) about the parameter time delay τ is obtained, as shown in Fig. 6 (g) and (h) through time series plot. The chaotic behaviour of the model is also shown through the bifurcation diagram 5 and through the phase portrait, shown in Fig. 7



(f). Figure 7 explains the dynamical behaviour of the model (8) for different values of τ according to the bifurcation diagram 5. These phase portraits clearly show that the behaviour of the solution of the model (8) changes with the parameter time delay τ . We have shown it clearly: as time delay increases, the unstable equilibrium becomes stable, showing the switching behaviour. For $\tau = 0.5$, a stable limit cycle is plotted in Fig. 7 (a) and (b). For $\tau = 2.5$, a stable spiral about the interior equilibrium is drawn. For $\tau = 6$, periodic doubling is plotted, with two types of cycles obtained for the same value. Finally, chaos is shown in Fig. 7 (f) for $\tau = 12$ using the phase portrait.



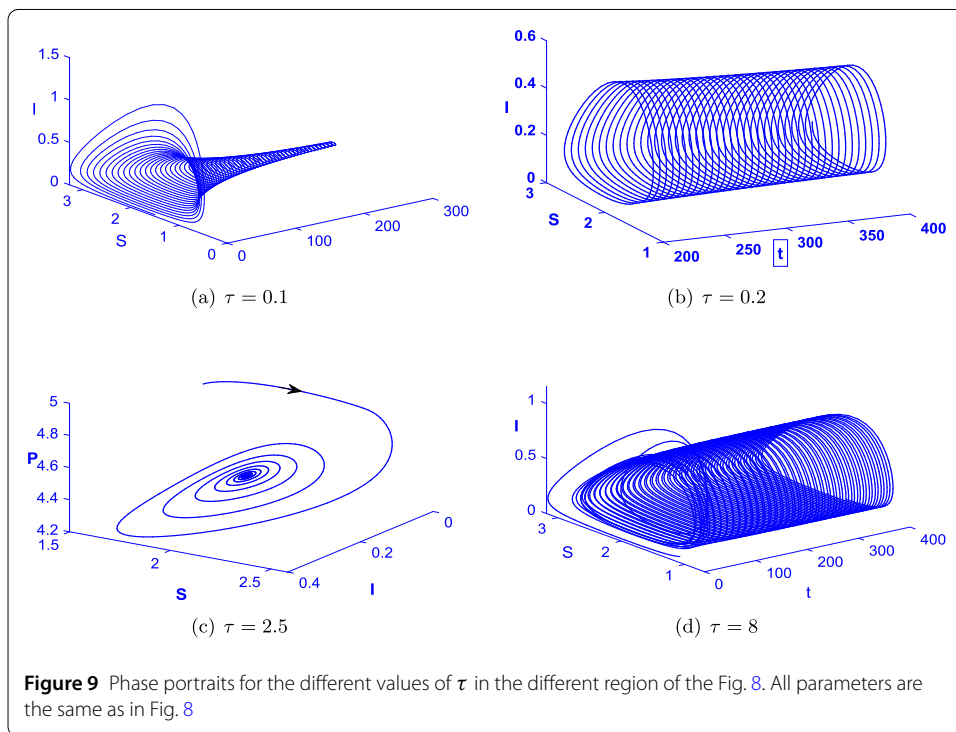
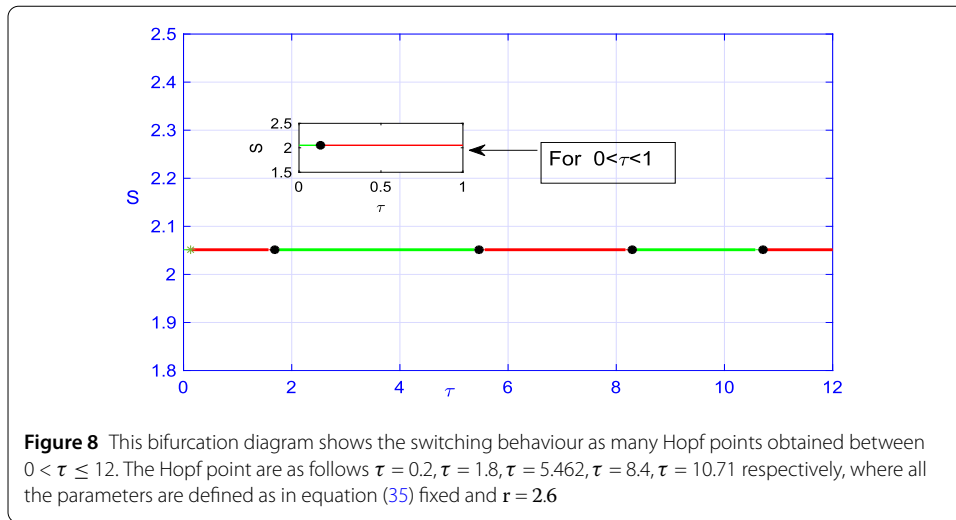
5.2.2 Impact of time delay on the model for the stable equilibrium

The time delay τ also impacts the stable equilibrium, as switching behaviour through the Hopf bifurcation appeared about the parameter τ shown in Fig. 8.

Figure 9 (a) shows a stable spiral equilibrium, Fig. 9 (b) shows a limit cycle, Fig. 9 (c) shows another stable spiral equilibrium, and Fig. 9 (d) shows a limit cycle or periodic behaviour. These phase portraits correspond to different bifurcation regions of Fig. 7.

6 Results and discussions

Time delay significantly impacts eco-epidemiological models, yielding more realistic results than non-delay models, as many ecological and biological processes inherently involve time delays. In this article, we analyse the existence and equilibrium points of both delay and non-delay models, along with their stability, using analytical and numerical methods. We observe that in the non-delay model, the interior equilibrium point exhibits switching behaviour with respect to parameter r . As depicted in Fig. 1, stability shifts from stable to unstable, then back to stable, and ultimately becomes unstable (oscillatory) as r increases. Figures 2 and 3 illustrate the stability and oscillatory behaviour of all species. Hopf bifurcation points are identified for Model (6) concerning the intrinsic growth rate parameter (r).



Model (6) with $\tau \neq 0$, shown in Model (8), experiences Hopf bifurcation regarding the time delay parameter τ , indicating that the time delay alters the system's stability. The model with time delay τ shows complex dynamics behaviour. As time delay induces Hopf bifurcation, periodic doubling and chaotic behaviour also show switching behaviour, as shown in Figs. 4 and 5 for the unstable equilibrium. The unstable equilibrium Model (6) becomes stable, periodic, and chaotic as time delay is incorporated. The time series plot 6 and corresponding phase portraits shown in Fig. 7 for different values of τ clearly describe the impact of time delay on the same. The periodic doubling and chaotic behaviour of the model (8) is shown through time series and phase portraits in Figs. 6 and 7. The equilibrium point, which is stable in the non-delay model, exhibits oscillatory and switching

behaviour as the time delay value increases, with multiple Hopf points obtained, as shown in Fig. 8. The phase portraits and time series demonstrate the stability and oscillatory behaviour of all species in the delay model for various bifurcation regions of τ . Figure 9 (a) and (c) depict the stable spiral interior equilibrium point, while Fig. 9 (b) and (d) show the oscillatory behaviour, respectively.

In the eco-epidemic model, incorporated with a time delay as a gestation delay, different dynamics are shown compared to the non-delay model. We discuss the impact of the gestation delay τ for both cases: stable and unstable equilibrium. Without gestation delay, the model has very simple dynamics, with only periodic solutions obtained in that case. However, in the case of the delay model, we have seen that the unstable equilibrium shows stable, oscillatory, periodic doubling, and chaotic behaviour with τ . Therefore, the time delay as gestation delay has a huge impact on the eco-epidemic model.

7 Conclusions

In conclusion, this study has thoroughly investigated the impact of time delay on eco-epidemiological models. The results show that the time delay significantly affects the stability and behaviour of the model, leading to complex dynamics, including Hopf bifurcation, periodic doubling, and chaotic behaviour. The incorporation of time delay as a gestation delay has been shown to alter the model's behaviour, leading to switching behaviour and multiple Hopf points. The study's findings highlight the importance of considering time delay in eco-epidemiological models, as it can significantly affect the model's predictions and realism. In future work, researchers may consider incorporating multiple time delay terms into the same model, such as maturation delay in prey growth, gestation delay in predators, and incubation delay in infected prey, further enhancing the model's realism and predictive capabilities.

Acknowledgements

Mr. Bipin Kumar acknowledges the fellowship from Council of Scientific and Industrial Research (CSIR) under Grant Number: 09/1278(12321)/2021-EMR-I.

Author contributions

The first author, BK, conceived the idea, conducted analyses and simulations, and drafted the manuscript. Mr. SH and RK Sinha conceptualized the flow for the entire draft of the manuscript, verified all the results, and edited the draft. All authors read and approved the final manuscript.

Funding

Not applicable.

Data availability

Not applicable.

Declarations

Competing interests

The authors declare no conflict of interest.

Author details

¹Department of Mathematics, National Institute of Technology Patna, Patna, Bihar 800005, India. ²Department of Applied Science and Humanities, Government Engineering College, Siwan, 841226, India.

Received: 23 July 2024 Accepted: 30 December 2024 Published online: 17 January 2025

References

1. Anderson, R.M., May, R.M.: Population biology of infectious diseases: part I. *Nature* **280**(5721), 361–367 (1979)
2. Anderson, R.M., May, R.M.: The invasion, persistence and spread of infectious diseases within animal and plant communities. *Philos. Trans. R. Soc. Lond. B, Biol. Sci.* **314**(1167), 533–570 (1986)

3. Bairagi, N., Roy, P.K., Chattopadhyay, J.: Role of infection on the stability of a predator-prey system with several response functions—a comparative study. *J. Theor. Biol.* **248**(1), 10–25 (2007)
4. Banerjee, M., Takeuchi, Y.: Maturation delay for the predators can enhance stable coexistence for a class of prey–predator models. *J. Theor. Biol.* **412**, 154–171 (2017)
5. Barman, B., Ghosh, B.: Role of time delay and harvesting in some predator-prey communities with different functional responses and intra-species competition. *Int. J. Model. Simul.* **42**(6), 883–901 (2022)
6. Basir, F.A., Tiwari, P.K., Samanta, S.: Effects of incubation and gestation periods in a prey–predator model with infection in prey. *Math. Comput. Simul.* **190**, 449–473 (2021)
7. Bélair, J., Campbell, S.A.: Stability and bifurcations of equilibria in a multiple-delayed differential equation. *SIAM J. Appl. Math.* **54**(5), 1402–1424 (1994)
8. Birkhoff, G., Rota, G.C.: *Ordinary Differential Equation, Stability and Complexity in Model Ecosystems*. Ginn, Boston (1982)
9. Chattopadhyay, J., Arino, O.: A predator-prey model with disease in the prey. *Nonlinear Anal.* **36**, 747–766 (1999)
10. Da Costa, R.E.P., Kinsman, R.H., Owczarczak-Garstecka, S.C., Casey, R.A., Tasker, S., Knowles, T.G., Woodward, J.L., Lord, M.S., Murray, J.K.: Age of sexual maturity and factors associated with neutering dogs in the uk and the republic of Ireland. *Vet. Rec.* **191**(6), Article ID e1265 (2022)
11. Dutta, P., Sahoo, D., Mondal, S., Samanta, G.: Dynamical complexity of a delay-induced eco-epidemic model with Beddington–DeAngelis incidence rate. *Math. Comput. Simul.* **197**, 45–90 (2022)
12. Enatsu, Y., Roy, J., Banerjee, M.: Hunting cooperation in a prey–predator model with maturation delay. *J. Biol. Dyn.* **18**(1), 2332279 (2024)
13. Gakkhar, S., Naji, R.K.: Seasonally perturbed prey–predator system with predator-dependent functional response. *Chaos Solitons Fractals* **18**(5), 1075–1083 (2003)
14. Geiger, M., Gendron, K., Willmitzer, F., Sánchez-Villagra, M.R.: Unaltered sequence of dental, skeletal, and sexual maturity in domestic dogs compared to the wolf. *Zool. Lett.* **2**, 1–8 (2016)
15. Ghosh, K., Samanta, S., Biswas, S., Rana, S., Elmojtaba, I.M., Kesh, D.K., Chattopadhyay, J.: Stability and bifurcation analysis of an eco-epidemiological model with multiple delays. *Nonlinear Stud.* **23**(2), 167–208 (2016)
16. Haldar, S., Khatua, A., Das, K., Kar, T.K.: Modeling and analysis of a predator–prey type eco-epidemic system with time delay. *Model. Earth Syst. Environ.* **7**, 1753–1768 (2021)
17. Hale, J.K., Verduyn Lunel, S.M.: *Introduction to Functional Differential Equations*. Springer, Berlin (1993)
18. Haque, M., Chattopadhyay, J.: Role of gestation delay in an eco-epidemic model with predator-prey interaction. *Math. Biosci.* **241**(2), 141–155 (2013)
19. Huang, C., Zhang, H., Cao, J., Hu, H.: Stability and Hopf bifurcation of a delayed prey-predator model with disease in the predator. *Int. J. Bifurc. Chaos* **29**(07), 1950091 (2019)
20. Hussain, S., Sen, M., Volpert, V.: Infection spreading in tissue as a reaction-diffusion wave. *Math. Med. Biol.* **41**(3), 169–191 (2024)
21. Hussien, R.M., Naji, R.K., et al.: The dynamics of a delayed ecoepidemiological model with nonlinear incidence rate. *J. Appl. Math.* **2023** (2023)
22. Jankovic, M., Petrovskii, S., Banerjee, M.: Delay driven spatiotemporal chaos in single species population dynamics models. *Theor. Popul. Biol.* **110**, 51–62 (2016)
23. Khajanchi, S.: Bifurcation analysis of a delayed mathematical model for tumor growth. *Chaos Solitons Fractals* **77**, 264–276 (2015)
24. Kumar, B.: Impacts of fisheries harvesting on fish–bird model for the Salton Sea region. *Commun. Math. Appl.* **15**(2) (2024)
25. Kumar, B., Sinha, R.K.: Dynamics of an eco-epidemic model with Allee effect in prey and disease in predator. *Comput. Math. Biophys.* **11**(1), 20230108 (2023)
26. Maiti, A.P., Jana, C., Maiti, D.K.: A delayed eco-epidemiological model with nonlinear incidence rate and Crowley–Martin functional response for infected prey and predator. *Nonlinear Dyn.* **98**, 1137–1167 (2019)
27. Pal, A.K., Bhattacharyya, A., Pal, S.: Study of delay induced eco-epidemiological model incorporating a prey refuge. *Filomat* **36**(2), 557–578 (2022)
28. Pandey, S., Das, D., Ghosh, U., Chakraborty, S.: Bifurcation and onset of chaos in an eco-epidemiological system with the influence of time delay. *Chaos, Interdiscip. J. Nonlinear Sci.* **34**(6), Article ID 063122 (2024)
29. Pati, N.C., Ghosh, B.: Delayed carrying capacity induced subcritical and supercritical Hopf bifurcations in a predator–prey system. *Math. Comput. Simul.* **195**, 171–196 (2022)
30. Perko, L.: *Differential Equations and Dynamical Systems*, vol. 7. Springer, Berlin (2013)
31. Rihan, F.A., et al.: *Delay Differential Equations and Applications to Biology*. Springer, Berlin (2021)
32. Roy, J., Dey, S., Banerjee, M.: Maturation delay induced stability enhancement and shift of bifurcation thresholds in a predator–prey model with generalist predator. *Math. Comput. Simul.* **211**, 368–393 (2023)
33. Saha, S., Maiti, A., Samanta, G.P.: A Michaelis–Menten predator–prey model with strong Allee effect and disease in prey incorporating prey refuge. *Int. J. Bifurc. Chaos* **28**(06), 1850073 (2018)
34. Saha, S., Samanta, G.P.: Analysis of a predator–prey model with herd behavior and disease in prey incorporating prey refuge. *Int. J. Biomath.* **12**(01), 1950007 (2019)
35. Saha, S., Samanta, G.P.: A prey–predator system with disease in prey and cooperative hunting strategy in predator. *J. Phys. A, Math. Theor.* **53**(48), 485601 (2020)
36. Schaller, G.B.: *The Serengeti Lion: A Study of Predator-Prey Relations*. University of Chicago Press, Chicago (2009)
37. Sharma, S., Samanta, G.P.: A Leslie–Gower predator–prey model with disease in prey incorporating a prey refuge. *Chaos Solitons Fractals* **70**, 69–84 (2015)
38. Srivastava, P.K., Banerjee, M., Chandra, P.: A primary infection model for hiv and immune response with two discrete time delays. *Differ. Equ. Dyn. Syst.* **18**, 385–399 (2010)
39. Thakur, N.K., Srivastava, S.C., Ojha, A.: Dynamical study of an eco-epidemiological delay model for plankton system with toxicity. *Iranian journal of science and technology. Trans A, Sci.* **45**(1), 283–304 (2021)
40. Upadhyay, R.K., Rao, V.S.H.: Impact of gestation delay on the stability of an eco-epidemic model with infected prey. *J. Biol. Syst.* **21**(2), 1350011 (2013)

41. Venturino, E.: Epidemics in predator models: disease among the prey. *Math. Popul. Dyn.: Anal. Heterog. Theor. Epid.* **1**, 381–393 (1995)
42. Venturino, E.: Epidemics in predator–prey models: disease in the predators. *Math. Med. Biol.* **19**(3), 185–205 (2002)
43. Verma, S.K., Kumar, B.: Bifurcation and pattern formation in a prey–predator model with cooperative hunting. *Eur. Phys. J. Plus* **139**(8), 1–20 (2024)
44. Xiao, Y., Li, M.: Effects of gestation delay on the dynamics of an eco-epidemic model with prey infection. *J. Math. Biol.* **66**(4), 731–753 (2013)
45. Yang, X., Chen, L., Chen, J.: Permanence and positive periodic solution for the single-species nonautonomous delay diffusive models. *Comput. Math. Appl.* **32**(4), 109–116 (1996)
46. Zhang, Z., Upadhyay, R.K., Agrawal, R., Datta, J.: The gestation delay: a factor causing complex dynamics in Gause-type competition models. *Complexity* **2018**(1), 1589310 (2018)
47. Zhou, X., Shi, X., Song, X.: Analysis of a delay prey-predator model with disease in the prey species only. *J. Korean Math. Soc.* **46**(4), 713–731 (2009)

Publisher's Note

Springer Nature remains neutral with regard to jurisdictional claims in published maps and institutional affiliations.

Submit your manuscript to a SpringerOpen[®] journal and benefit from:

- Convenient online submission
- Rigorous peer review
- Open access: articles freely available online
- High visibility within the field
- Retaining the copyright to your article

Submit your next manuscript at ► [springeropen.com](https://www.springeropen.com)
